Near Infrared Photoimmunotherapy Targeting DLL3 For Small Cell Lung Cancer

Yoshitaka Isobe[a], Kazuhide Sato*[a,b,c], Yuko Nishinaga[a], Kazuomi Takahashi[a], Shunichi Taki[a], Hirotoshi Yasui[a], Misae Shimizu[a,c], Rena Endo[a,c], Chiaki Koike[a,c], Noriko Kuramoto[c], Hiroshi Yukawa[c,d,e], Shota Nakamura[f], Takayuki Fukui[f], Koji Kawaguchi[f], Toyofumi F. Chen-Yoshikawa[f], Yoshinobu Baba[d,e], Yoshinori Hasegawa[g]

[a] Respiratory Medicine, Nagoya University Graduate School of Medicine

[b] Nagoya University Institute for Advanced Research, S-YLC

[c] Nagoya University Institute for Advanced Research, B3-Unit, Advanced Analytical and Diagnostic Imaging Center (AADIC) / Medical Engineering Unit (MEU)

[d] Nagoya University Institute of Nano-Life-Systems, Institutes of Innovation for Future Society

[e] Department of Biomolecular Engineering, Nagoya University Graduate School of Engineering

[f] Department of Thoracic Surgery, Nagoya University Graduate School of Medicine

[g] National Hospital Organization, Nagoya Medical Center

*Correspondence should be addressed to: Kazuhide Sato, M.D., Ph.D.

Institute for Advanced Research, Department of Respiratory Medicine, Graduate School of Medicine, Nagoya University, Nagoya, Aichi, 466-8550, Japan.

Phone: +81-52-744-2167; Fax: +81-52-744-2176; E-mail: k-sato@med.nagoya-u.ac.jp

ABSTRACT

Background

Small cell lung cancer (SCLC) has a poor prognosis, and its treatment options are limited. Delta-like protein 3 (DLL3) is expressed specifically in SCLC and is considered a promising therapeutic target for patients with this disease. Rovalpituzumab tesirine (Rova-T) was the first antibody-drug conjugate targeting DLL3. Although Rova-T development was unfortunately terminated, DLL3 remains an ideal target for SCLC. Near infrared photoimmunotherapy (NIR-PIT) is a new form of cancer treatment that employs an antibody-photosensitiser conjugate followed by NIR light exposure and damage target cells specifically. In this study, we demonstrate DLL3-targeted NIR-PIT to develop a novel molecularly targeted treatment for SCLC.

Methods

The anti-DLL3 monoclonal antibody rovalpituzumab was conjugated to an IR700 photosensitiser (termed 'rova-IR700'). SCLC cells overexpressing DLL3 as well as non-DLL3-expressing controls were incubated with rova-IR700 and then exposed to NIR-light. Next, mice with SCLC xenografts were injected with rova-

IR700 and irradiated with NIR-light.

Findings

DLL3-overexpressing cells underwent immediate destruction upon NIR-light exposure, whereas the control cells remained intact. The xenograft in mice treated with rova-IR700 and NIR-light shrank markedly, whereas neither rova-IR700 injection nor NIR-light irradiation alone affected tumour size.

Interpretation

Our data suggest that targeting of DLL3 using NIR-PIT could be a novel and promising treatment for SCLC.

Funding

Research supported by grants from the Program for Developing Next-generation Researchers (Japan Science and Technology Agency), KAKEN (18K15923, JSPS), Medical Research Encouragement Prize of The Japan Medical Association, The Nitto Foundation, Kanae Foundation for the Promotion of Medical Science.

Keywords: photoimmunotherapy, DLL3, small cell lung cancer, bioluminescence, *in vivo* imaging

Abbreviations

BLI, bioluminescence imaging; DLL3, delta like protein 3; LCNEC, large cell neuroendocrine carcinoma; NIR, near infrared; PIT, photoimmunotherapy; Rova-T, rovalpituzumab tesirine.

Research in context

Evidence before this study

Small cell lung cancer (SCLC) has a poor prognosis, and its treatment options are very limited. Moreover, molecularly targeted therapy for SCLC have not yet successfully been implemented. Recent studies have revealed that DLL3 is specifically expressed in SCLC, and it is an ideal molecular target. Thus, the antibody drug conjugate targeting DLL3, Rovalpituzumab tesirine (Rova-T) has developed into the phase III clinical trials with much expectation. However, unfortunately the results of the trials have failed recently. Although Rova-T development has been discontinued, DLL3 is still a good molecular target for SCLC. Therefore, the enhancement therapies targeting DLL3 with an innovative technique are required.

Near infrared photoimmunotherapy (NIR-PIT) is a new form of cancer treatment that employs an antibody photosensitiser conjugate followed with NIR-light exposure. The cytotoxicity by NIR-PIT has uniqueness

of very rapid necrosis, which is totally different from other anti-cancer therapies. Recently the cell death mechanism has been clarified that the photo-chemical reaction induces acute molecular change of hydrophilic state into hydrophobic, resulting in cancer cell membrane damages. NIR-PIT has been under the Phase III trials with US-FDA fast track, and expected to be approved in a few years.

Added value of this study

We found high DLL3-expression in SCLC clinical resected specimens in our institute. Moreover, we confirm the high DLL3-expression in not only Caucasian SCLC cell lines but also Japanese SCLC cell lines, in addition, not in the normal lung epithelial cell lines.

To enhance the antitumour-effect targeting DLL3, we exploited NIR-PIT for SCLC. We demonstrated DLL3-targeted NIR-PIT with Rovalpituzumab, which is the same monoclonal humanised antibody as the usage in the previous clinical trials, *in vitro* and *in vivo*. DLL3-targeted NIR-PIT damages only DLL3 expressing cells, and non-target cells remains intact *in vitro* assessment, and significantly inhibited the growth of SCLC and improved survival in a mouse model.

Implications of all the available evidence

This study provides the evidence that DLL3 is specifically and widely expressing in SCLC patients in Japanese, and the universality of the DLL3-expression between Caucasian and Japanese SCLC patients. Moreover, in vivo data give the proof of the concept that DLL3-targeted NIR-PIT for SCLC patients will be a promising new treatment. Since NIR-PIT is undergoing an international phase III clinical trial, and Rova-T has terminated the phase III, DLL3-targeted NIR-PIT is thought to be easy translatable into the clinic.

1. Introduction

Small cell lung cancer (SCLC), which accounts for 15% of lung malignancies, has a poor prognosis[1]. SCLC is often discovered after it is already at an advanced, unresectable stage, and treatment is thus limited to anticancer drug therapy. While novel tyrosine kinase inhibitors and immune checkpoint blockers are continuously being developed for non-SCLCs, treatment options for SCLCs have not advanced for 2–3 decades[2].

Delta-like protein 3 (DLL3) is a potential therapeutic target molecule for SCLC. It was originally identified as a ligand for the notch signaling pathway[3], but was more recently found to be highly

expressed in SCLC and not in adult tissues[4,5]. Rovalpituzumab tesirine (Rova-T) was the first antibody-drug conjugate (ADC) targeting DLL3. However, **TAHOE** (NCT03061812) and **MERU** (NCT03033511) trials could not meet their primary objective, and Rova-T development was terminated on August 2019. DLL3 remains ideal target for SCLC regardless of the trial results, new approach is needed.

Near infrared (NIR) photoimmunotherapy (PIT) is a new form of cancer therapy that employs an antibody photosensitiser conjugate followed by NIR light exposure[6]. An antibody photosensitiser conjugate consists of a cancer cell-specific monoclonal antibody (mAb) and a photosensitiser, IR700, which is a silica-phthalocyanine derivative that is covalently conjugated to the antibody[7]. It binds target molecules on the cell membrane and induces immediate cell necrosis after exposure to NIR light at 690 nm[8–10]. This new therapy is now undergoing an international phase III clinical trial against locoregional, recurrent head and neck squamous cell carcinoma (HNSCC) (**LUZERA-301**, NCT03769506). With fast track designation by the United States Food and Drug Administration (US-FDA), NIR-PIT is expected to gain approval in a few years.

Among the organs in the body, the lung can transmit NIR light most effectively because it comprises a large amount of air[11,12]. Thus, thoracic cancers including SCLC are potential targets for NIR-PIT. Herein, we employed NIR-PIT to develop a novel phototherapy modality for SCLC using rovalpituzumab, the anti-DLL3 mAb, and performed a preclinical evaluation of the resulting conjugate.

2. Materials and methods

2.1. Study design

Our research objective was to establish a new treatment for SCLC using NIR-PIT. All *in vivo* procedures were conducted in compliance with the Guide for the Care and Use of Laboratory Animal Resources of Nagoya University Animal Care and Use Committee (approval #00238). The ethical board of Nagoya University, Clinical Research Committee, approved the use of materials from the patients (approval #2018-0046). The patients were consented with the use of their resected tumour samples, and informed that they could withdraw consent at any time.

2.2. Immunostaining of surgically resected SCLC/large cell neuroendocrine carcinoma (LCNEC)/carcinoid cell specimens

We performed immunostaining of DLL3 in the resected specimens of Japanese patients pathologically diagnosed with SCLC, LCNEC, or lung carcinoids who underwent surgery at Nagoya University Hospital between April 2004 and December 2015. Four micrometer-thick sections were produced from formalin-

fixed, paraffin-embedded tumour samples and placed on glass slides. Epitope retrieval was performed using a pH 9 buffer (Epitope Retrieval Solution pH 9; Leica Biosystems, Nussloch, Germany) and a pressure cooker. We used rabbit polyclonal anti-DLL3 antibody (1:1000; Delta3/DLL3 IHC-plus™; LS Bio, Seattle, WA, USA) and horseradish peroxidase-polymer secondary antibody (EnVision+ system HRP-labelled polymer anti-rabbit; Agilent, Santa Clara, CA, USA). Colorimetric development was performed with 3,3′-diaminobenzidine (ImmPACT DAB Substrate; Vector, Burlingame, CA, USA) and hematoxylin. DLL3 expression was evaluated at 100× and 400× magnification under a brightfield microscope. Positive staining was defined as the staining of 1% or more of the tumour cell at any intensity, whether cytoplasmic or membranous, based on previous guidance[13].

2.3. Reagents

The water-soluble, silica-phthalocyanine derivative IRDye 700DX N-hydroxysuccinimide (NHS) ester was purchased from LI-COR Biosciences (Lincoln, NE, USA). Rovalpituzumab was obtained from Creative Biolabs (Shirley, NY, USA). All other chemicals were of reagent grade.

2.4. Cell lines

SBC3 and SBC5 cell lines, both derived from Japanese patients with SCLC, were obtained from the Japanese Collection of Research Bioresources (Osaka, Japan); 3T3 (mouse fibroblast) (ATCC Cat# CRL-1658, RRID:CVCL_0594), H69 (human SCLC) (ATCC Cat# HTB-119, RRID:CVCL_1579), and H82 (human SCLC) (ATCC Cat# HTB-175, RRID:CVCL_1591) cells were obtained from the American Type Culture Collection (Manassas, VA, USA). The *cdk4*/*hTERT*-immortalised normal human bronchial epithelial cell line HBEC3 was obtained from Hamon Center collection (University of Texas Southwestern Medical Center, Dallas, TX, USA)[14].

DLL3, green fluorescent protein (GFP), and luciferase-expressing SBC5 and 3T3 cell lines were established by transfecting RediFect Red-FLuc lentiviral particles (PerkinElmer, Waltham, MA, USA) and DLL3-GFP lentiviral particles (OriGene, Rockville, MD, USA). Balb/3T3 cells stably expressing red fluorescent protein (RFP) were established by transfection with RFP (EF1a)-puro lentiviral particles (AMSBIO, Cambridge, MA, USA)[11,12,15]. Stable, high expression of DLL3, GFP, luciferase, or RFP was confirmed after performing more than 10 cell passages. We referred to DLL3, GFP, and luciferase-expressing SBC5/3T3 as SBC5-DLL3-luc-GFP/3T3-DLL3-luc-GFP, and to RFP-expressing 3T3 as 3T3-RFP. H69/cisplatin (CDDP)[16] and H69/vePesid (VP)[17] were obtained from Kindai University (Dr. Nishio Kazuto), while SBC3/CDDP[18], SBC3/etoposide (ETP)[19], and SBC3/7-ethyl-10-hydroxycamptothecin (SN38)[20] were obtained from Okayama University (Dr. Kiura Katsuyuki). Note that '/[drug]' indicates

resistance to that drug.

2.5. Cell culture

Cells were all cultured in RPMI 1640 medium (Thermo Fisher Scientific, Rockford, IL, USA) supplemented with 10% fetal bovine serum and penicillin (100 IU/mL) and streptomycin (100 mg/mL) (Thermo Fisher Scientific).

2.6. Synthesis of IR700-conjugated rovalpituzumab

Rovalpituzumab (1 mg, 6.8 nmol) was incubated with IR700 NHS ester (LI-COR Biosciences, Lincoln, NE, USA) (66.8 mg, 34.2 nmol, 5 mmol/L in DMSO) in 0.1 mol/L Na_2HPO_4 (pH 8.6) at room temperature for 1 hour. The mixture was purified using a Sephadex G50 column (PD-10, GE Healthcare; Piscataway, NJ, USA). The protein concentration was determined using a Coomassie Plus protein assay kit (Thermo Fisher Scientific) by spectroscopically measuring the absorption at 595 nm (Novaspec Plus; GE Healthcare). The concentration of IR700 was measured via absorption at 689 nm using spectroscopy to confirm the number of mAb-conjugated fluorophores. The synthesis was controlled so that an average of 3 IR700 molecules were bound to a single antibody; these rovalpituzumab conjugates are referred to as rova-IR700.

2.7. SDS-PAGE and immunoblotting

We performed quality control for the conjugate using SDS-PAGE as previously described[21]; diluted rovalpituzumab was used as a non-conjugated control. The fluorescent bands were measured with an Odyssey Imager (LI-COR Biosciences) using a 700 nm fluorescence channel.

Immunoblotting was performed to confirm specific binding to DLL3. For western blot analysis, lysates from transiently DLL3-overexpressing cells as well as control lysates (OriGene) were separated by SDS-PAGE. Proteins were transferred to nitrocellulose membranes, blocked in BlockOne (Nacalai Tesque, Kyoto, Japan), incubated with rova-IR700, and detected via fluorescence using an Odyssey Imager (700 nm fluorescence channel).

2.8. Flow cytometry

Flow cytometry was performed to evaluate DLL3 expression in the cell lines. Two hundred thousand cells were seeded into 12-well plates and incubated with rova-IR700 at 10 μg/mL for 12 hours at 37°C. The medium was replaced with PBS after washing twice with the same. To avoid affecting antigen-antibody reaction with trypsin, the cells were detached from the wells by pipetting, and IR700 fluorescence was evaluated in 10,000 cells using a flow cytometer (Gallios, Beckman Coulter). To evaluate specific binding

to DLL3, a block study was performed with SBC3 cells that were incubated with excess rovalpituzumab beforehand. HBEC3 cells were incubated with CD16 antibody (10 μg/mL; CD16/CD32 mAb [clone 93], Thermo Fisher Scientific) for 6 hours before assaying to evaluate DLL3 expression as evidenced by binding to the Fab region of rovalpituzumab.

2.9. Fluorescence microscopy

To detect the antigen-specific localization of IR700 conjugates, observation with fluorescence microscopy was performed (A1Rsi and TiE-A1R, Nikon Instech, Tokyo, Japan). Ten thousand cells were seeded on cover glass-bottomed dishes and incubated for 6 hours. Rova-IR700 was then added to the culture medium at 10 μg/mL and incubated at 37°C for 12 hours. The cells were then washed with PBS twice. Propidium iodide (PI, 1:2,000; Thermo Fisher Scientific) and Sytox Blue (1:500; Thermo Fisher Scientific) were added to the media 30 minutes before observation to stain the dead cells. The cells were then exposed to NIR light (4 J/cm^2) and serial microscopic images were obtained.

2.10. *In vitro* NIR-PIT

Two hundred thousand cells were seeded into 12-well plates and incubated with rova-IR700 at 10 μg/mL for 12 hours at 37°C. The medium was replaced with PBS after washing twice with the same. The cells were irradiated with an NIR light-emitting diode, which emits light at a wavelength of 670–710 nm (L690-66-60; Ushio-Epitex, Kyoto, Japan). The actual power density (mW/cm^2) was measured with an optical power meter (PM100; Thorlabs, Newton, NJ, USA).

2.11. Cytotoxicity/phototoxicity assay

The *in vitro* cytotoxic effects of NIR-PIT with rova-IR700 were determined via luciferase activity as well as PI staining using flow cytometry. For luciferase activity, 200 μL of 150 μg/mL of D-luciferin-containing media (GoldBio, St Louis, MO, USA) was administered to PBS-washed cells 24 hours after NIR-PIT; the cells were then analyzed on a bioluminescence plate reader (Powerscan4; BioTek, Winooski, VT, USA). We evaluated luciferase activity *in vitro* 1, 3, 6, and 24 hours after NIR light exposure. With this estimation, we decided to evaluate luciferase activity *in vitro* at 24 hours after NIR-PIT. For the flow cytometric assay, cells were dissociated at 1 hour after treatment and washed with PBS twice. The cells were detached from the wells by pipetting, and PI was added to the cell suspension (final concentration, 2 μg/mL) and incubated at room temperature for 30 minutes before performing flow cytometry. PI fluorescence in 10,000 cells was measured using FACS Calibur (Becton Dickinson, Franklin Lakes, NJ, USA).

2.12. Animal and tumour models

All *in vivo* procedures were conducted in compliance with the local Animal Care and Use Committee of Nagoya University. Eight to 12-week-old female homozygote athymic nude mice were purchased from Chubu Kagaku Shizai (Nagoya, Japan). The mice were housed in temperature-controlled rooms with a 12h light / 12h dark cycle at Division of experimental Animals of Nagoya University. The animals were maintained and bred under antigen and virus free conditions, and fed on a white-colored food diet for at least 1 week before investigation to minimize the fluorescence from diet. The mice were anesthetised with isoflurane before conducting any procedures. Appropriate experimental sample size was estimated from previous studies. Six million SBC5-DLL3-luc-GFP cells were injected subcutaneously into one or both sides of the dorsum. To determine tumour volume, the greatest longitudinal diameter (length) and the greatest transverse diameter (width) were measured with an external caliper. Tumour volumes based on caliper measurements were calculated using the following formula: tumour volume = length × width^2 × 0.5. Tumours reaching approximately 200 mm^3 in volume were selected for the experiment. Rodents with suitable tumour sizes and bioluminescence signals were selected for further investigation. The mice were sacrificed using carbon dioxide asphyxiation when tumours exceeded 15 mm in length.

2.13. *In vivo* bioluminescence imaging (BLI)

D-luciferin (15 mg/mL, 200 μL) was injected intraperitoneally 13 days after cell implantation for purposes of BLI, and the mice were analyzed on an IVIS imaging system (Perkin Elmer) for luciferase activity. Regions of interest were identified on the tumours from which to quantify the bioluminescence.

2.14. *In vivo* fluorescence imaging

IR700 fluorescence images were acquired before and after therapy with a fluorescence imager (Pearl Imager, LI-COR Biosciences).

2.15. *In vivo* local DLL3-targeted NIR-PIT

Mice with a single-dorsum xenograft were randomised into 4 groups as follows: (1) no treatment (control); (2) only NIR light exposure (light only); (3) rova-IR700 injection without NIR light irradiation (i.v. only); (4) rova-IR700 injection followed with NIR light irradiation (PIT). The mice were injected with 50 μg of rova-IR700 on day -1 (13 days after tumour cell inoculation into the mice) and irradiated with NIR light at 50 J/cm^2 on day 0 and again at 100 J/cm^2 on day 1. Mice with 2 dorsal tumours were injected with 50 μg of rova-IR700 on day -1, and the larger tumour was irradiated with NIR light at 100 J/cm^2 on day 0.

2.16. Statistics

Data are expressed as means ± SEM of a minimum of 3 experiments unless otherwise indicated. Statistical analyses were performed using the Prism software (GraphPad, San Diego, CA, USA). For 2-group comparisons, the Mann-Whitney test or Student's t-test was used. For multiple-group comparisons, a 1-way ANOVA with Tukey's test or Kruskal-Wallis test with Dunn's test was used. The cumulative probability of survival, defined as the non-achievement of a tumour diameter of 15 mm, was estimated in each group using Kaplan-Meier analyses, and the results were compared with log-rank and Wilcoxon tests. p-values <0.05 were considered indicative of statistically significant differences.

3. Results

3.1. Immunostaining of human resected SCLC, LCNEC, and carcinoid cell surgical specimens

DLL3 is considered to express widely in neuroendocrine tumours[22], and we planned to evaluate whether DLL3 is expressed in Japanese SCLC, LCNEC, and carcinoids (other than NSCLC). Ten SCLC, 10 LCNEC, and 8 carcinoid samples were obtained and stained using the same protocol for all. Samples were evaluated by 3 medical doctors. Eight of 10 SCLCs, 5 of 10 LCNECs, and all 8 carcinoid samples were DLL3-positive (**Fig. 1a, b**). The DLL3 positivity rate for SCLCs was consistent with those of previous reports[13,23]. These data supported the rationale to develop DLL3-targeted NIR-PIT.

3.2. Conjugation of the anti-DLL3 mAb with IR700DX

The integrity of the rova-IR700 conjugate was confirmed after observing strong binding between the mAb and IR700, while rovalpituzumab alone had no detectable fluorescent signals on SDS-PAGE (**Fig. 2a**). Binding of rova-IR700 to the DLL3 receptor antigen was examined by immunoblotting lysates from cells transiently overexpressing DLL3 (**Fig. 2b**). During flow cytometric assays, SBC3 signals were blocked following the addition of excess rovalpituzumab; almost no signals were observed in either the human normal bronchial epithelial cell line HBEC3 (**Fig. 2c**) or 3T3 mouse fibroblasts (**Supplementary Fig. 1**). Collectively, these results indicate that rovalpituzumab and IR700 were successfully conjugated, and that rova-IR700 could specifically bind to DLL3.

3.3. *In vitro* characterization of the specific binding of rova-IR700 to DLL3

To confirm the effect of DLL3-targeted NIR-PIT using optical monitoring, the SCLC cell line SBC5 as well as mouse fibroblast 3T3 cells were genetically modified to express DLL3, GFP, and luciferase (SBC5-DLL3-luc-GFP and 3T3-DLL3-luc-GFP) (**Supplementary Fig. 2a, b**). As a non-target control of NIR-PIT,

the 3T3 cell line was optically modified to express RFP (3T3-RFP)[12,24].

The fluorescent signals obtained with rova-IR700 from SBC3/SBC5 (Asian patient-derived SCLC cell lines), H69/H82 (Caucasian patient-derived SCLC cell lines), SBC3/CDDP, SBC3/ETP, SBC3/SN38, H69/CDDP, and H69/VP (the chemo-agent-resistant SCLC cell lines) were evaluated using flow cytometry. Fluorescent signals from SBC3 or SBC5 cells exhibited similar intensity as those from H69 and H82 cells (**Fig. 3a**). Moreover, chemoresistant cell lines showed almost the same signal intensity as those of their parent cells (**Fig. 3b**). These data indicated that DLL3 is widely expressed in SCLC cell lines regardless of the race of the patients of origin or previous chemotherapy treatment status.

3.4. *In vitro* NIR-PIT effects with rova-IR700 in SCLC cell lines

Serial observation of SBC5-DLL3-luc-GFP and 3T3-DLL3-luc-GFP cells was performed using a fluorescence microscope before and after NIR-PIT. After exposure to NIR light (4 J/cm^2), cellular swelling, bleb formation, and death were observed (**Fig. 4a**). Time-lapse image analysis showed acute morphologic changes in the cell membrane as well as PI fluorescence, which indicated necrotic cell death (**Supplementary Video 1a, b**). Moreover, the DLL3-GFP fluorescence disappeared concomitantly with the loss of IR700 fluorescence. Most of these cellular changes were observed within 30 minutes after light exposure, indicating a rapid induction of necrotic cell death after NIR-PIT. No significant changes were observed in DLL3-negative 3T3-RFP cells, suggesting NIR-PIT induced no damage on nontarget cells (**Fig. 4b, Supplementary Video 2**).

Next, to quantitate the effect of NIR-PIT *in vitro*, we performed a cytotoxicity assay 1 hour after NIR light irradiation using PI staining as well as 24 hours later using luciferase activity quantitation. The proportion of dead cells (as determined by PI incorporation) increased in a light dose-dependent manner. No significant cytotoxicity was observed with NIR light exposure alone or rova-IR700 alone (**Fig. 4b**). Luciferase activity showed significant decreases in relative light units from NIR-PIT-treated cells (**Fig. 4c**). Collectively, these experiments confirmed that NIR-PIT causes necrotic cell death in a light dose-dependent manner *in vitro*.

3.5. *In vivo* biodistribution of rova-IR700 in tumour bearing mice

To examine the distribution of rova-IR700 *in vivo*, we used a xenograft model in which SBC5-DLL3-luc-GFP cells were introduced into the right dorsum of mice. After fifty micrograms of rova-IR700 injection, high fluorescence was observed across the entire mouse's body; then, the tumour was gradually visualised over the following 2 hours (**Fig. 5a**). High-intensity fluorescence was observed immediately after injection and on day 1, while the highest tumour-to-background ratio was observed on days 2–3 (**Fig. 5b, c**). There was no other specific localization of IR700 except in the liver and bladder presumably owing to hepatic

metabolism and urinary excretion. The accumulation in the tumour and liver was confirmed with *ex vivo* imaging. IR700 fluorescence was observed in the tumours and livers of injected mice but not in other organs, and was entirely absent in non-injected mice (**Fig. 5d**). These results indicate that rova-IR700 was distributed specifically in DLL3-expressing tumours, and that treatments 1 and 2 days after rova-IR700 administration were appropriate.

3.6. *In vivo* anti-tumour effect of DLL3-targeted NIR-PIT.

To monitor targeted tumour cell destruction induced by NIR-PIT, BLI and fluorescence from mice with tumours in the right dorsum were examined (**Fig. 6a**). IR700 fluorescence from the tumour decreased after NIR light irradiation. Luciferase activity in the control, light-only, and rova-IR700 groups, as determined by BLI, showed a gradual increase concomitant with tumour growth. In contrast, luciferase activity gradually decreased during the 2 days after NIR-PIT (**Fig. 6b**). NIR-PIT introduced on days 0 and 1 led to significant reductions in the proportions of tumour volumes whereas neither rova-IR700 injection nor NIR light irradiation alone affected tumour size. (PIT group vs. control group at day 3: *p = 0.0212; PIT group vs. control group at day 7: *p = 0.0084; PIT group vs. light only group at day 7: *p = 0.0123; PIT group vs. light only group at day 10: *p = 0.0136; light only group vs. control group at day 3, 7, 10: p > 0.9999; i.v. only group vs. control group at day 3, 7, 10: p > 0.9999, Kruskal-Wallis test with Dunn's post-test) (**Fig. 6c**). Quantitative relative light unit measurement showed a significant decrease in NIR-PIT-treated tumours (PIT group vs. light-only group in (b): *p = 0.0007; PIT group vs. control group at (c): *p = 0.0385, Kruskal-Wallis test with Dunn's post-test) (**Fig. 6d**). Survival was observed up to 70 days after cell injection. Survival was significantly prolonged in the NIR-PIT group (*p = 0.023, log-rank test) (**Fig. 6e**). The changes in the body weights of the mice were negligible throughout the experiment (**Supplementary Fig. 3**), suggesting that the therapy does not cause general adverse effects. Next, we examined the site-specific effects of DLL3-targeted NIR-PIT in the same mice. With dual dorsal flank tumour model, IR700 fluorescence disappeared only at the treated site immediately after NIR-PIT, while the internal luminescence of the treated tumour disappeared 1 day after NIR-PIT (**Fig. 6f, g**). Taken together, DLL3-targeted NIR-PIT was effective against the flank tumour and successfully achieved site-specific ablation.

4. Discussion

In this study, we demonstrated DLL3-targeted NIR-PIT. *In vitro* assessment revealed that SCLC cell lines derived from both Caucasian and Japanese patients express DLL3. Immunostaining of resected SCLC, LCNEC, and carcinoid specimens from patients treated at our institution also confirmed that DLL3 was commonly and widely expressed. Therefore, DLL3 appears to be a promising target for anti-SCLC

therapies. As such, we demonstrated the combination of NIR-PIT technology and rovalpituzumab, which was recently developed as a humanised mAb[5,25]. DLL3-targeted NIR-PIT damages DLL3 expressing target cell but not non-target cell *in vitro*. Upon *in vivo* assessment, the treatment significantly and selectively inhibited the growth of SCLC in a mouse model. DLL3-targeted NIR-PIT in a mouse model also prolonged the survivals. Moreover, since the anticancer drug Rova-T was already subjected in its first in human clinical trial[13], NIR-PIT with rovalpituzumab can easily be translatable into the clinic.

The available therapeutic options for SCLC have not changed in decades[1]. The standard first-line chemotherapy is the combination of a platinum salt with a second agent, while the only second-line chemotherapy approved by the US-FDA is topotecan; there are no approved third-line treatments[2]. Nowadays, many molecular-targeted therapies such as poly (ADP-ribose) polymerase inhibitors (e.g. Veliparib)[26,27], Wee1 inhibitors (e.g. AZD1775)[28,29], or enhancer of zeste homolog 1 or 2 inhibitors (e.g. Tazometostat)[30,31] have been developed against SCLC[2]; however, these fall short in terms of efficacy. Another method of targeting SCLC using mAbs for cell surface markers such as neural cell adhesion molecule (NCAM), trophoblast cell-surface antigen 2 (TROP-2), epithelial cell adhesion molecule (EpCAM), and DLL3[32]. Among these, DLL3 was originally identified as an inhibitor of the tumour-suppressor NOTCH1 in SCLC[2,33]. Recent studies revealed that the high expression of DLL3 promotes cell growth and fission as well as a reduction in apoptosis[34,35]. While DLL3 is expressed in few non-SCLCs, it is reportedly overexpressed in 82.5% of SCLCs; moreover, another study found that 31.7% of SCLC specimens were found to exhibit high DLL3 expression in ≥50% of the tumour cells[5,23].

Rova-T was developed as an ADC that targets DLL3 and was effective in SCLC cell cultures and 'patient-derived xenograft' mouse models[5]. In a previous clinical trial, Rova-T treatment produced overall response rates of 38% and 0% in patients with DLL3-high (i.e. ≥50% expression) and DLL3-low (i.e. <50% expression) tumours, respectively[13]. In the phase II TRINITY trial which assessed safety and efficacy in the third-line and beyond setting for patients with DLL3-expressing SCLC, Rova-T showed modest clinical activity[36]. The TAHOE phase III trial compared Rova-T to the current standard agent (topotecan) as a second-line treatment for SCLC (NCT03061812), but was halted owing to inferior outcomes in patients of the Rova-T arm. Additionally, the MERU phase III trial evaluating Rova-T as a first-line maintenance therapy for advanced SCLC demonstrated no survival benefit at a pre-planned interim analysis, and the trial has been closed (NCT03033511). These results suggest that SCLC treatment targeting DLL3 should be modified to improve combination chemotherapies or to expand NIR-PIT technology.

NIR-PIT is a highly specific anticancer therapeutic modality that is being tested in a few clinical trials[37]. LUZERA-301 is an ongoing phase III randomised, double-arm, open-label, controlled trial comparing ASP-1929 photoimmunotherapy to the current standard of care for locoregional recurrent HNSCC in

patients who have failed at least two lines of therapy. ASP-1929 is a conjugate of cetuximab and IR700 targeting the epidermal growth factor receptor and has received 'fast track' designation by the US-FDA for the treatment of HNSCC. The result of the phase II trial was promising; hence, NIR-PIT is expected to be approved and available in the near future.

The mechanism of NIR-PIT was unclear for years, as it does not damage normal tissues but only targets cells if the appropriate light source and specific antigen/antibody combinations are available[6,12,24]. A recent study aimed at identifying the mechanism of NIR-PIT found that photochemical ligand reactions are critical drivers of rapid necrotic cell death[38]. This reaction converts the hydrophilic side chains of IR700 to hydrophobic variants that render the antibody-IR700 conjugates insoluble; this reduces cell membrane integrity and allows the surrounding aqueous fluid to flow in[38]. This photochemical reaction-induced cell death is therefore a new concept in cytotoxicity that demonstrates the uniqueness of NIR-PIT therapy.

There are a few concerns when using this treatment. First, NIR-PIT can only be used locally, and second, there are no established light sources that can deliver sufficient NIR light to human lungs. Approximately 70% of SCLCs are found to be 'extensive stage' types at the diagnosis[39], for which new treatments are required. However, there exist preclinical reports of NIR-PIT targeting lung metastases[40], or used with ADCs[41], chemotherapy[42], immune checkpoint inhibitors[43], and anti-regulatory T-cell therapies[44]; these may be effective against extensive-stage SCLC. Thus, the aforementioned concerns could be outweighed by introducing such combination therapies. Moreover, the fact that Rova-T has been used as a DLL3-targeting ADC in clinical studies indicates that the combination of NIR-PIT and Rova-T may be easily translatable into the clinic. For example, the primary tumours can be irradiated using NIR-PIT while metastatic small lesions can be treated with tesirine, the anti-cancer drug of Rova-T.

Currently, external light from light-emitting diodes, lasers[45], and optical fibres[46] are being used as light sources. When targeting inner organ lesions, irradiation via the digestive tract, arteries, or even implantable devices might become possible with or without external irradiation. There are already some reports of light sources attached to endoscopes[47] and implantable devices[48].

In conclusion, NIR-PIT targeting DLL3 to treat SCLC was very feasible and showed marked antitumour effects. As such, NIR-PIT targeting DLL3 could be a promising treatment for SCLC.

Acknowledgement

We would like to thank all the members of our laboratory and section for their comments and suggests on this research. We also thank to the nano-plat form at Nagoya University, and core technical staffs in Nagoya University Equipment Sharing System.

Funding Sources

This research was supported by the Program for Developing Next-generation Researchers (Japan Science and Technology Agency), KAKEN (18K15923, JSPS), Konica Minolta Science and Technology Foundation, Medical Research Encouragement Prize of The Japan Medical Association, The Uehara Memorial Foundation, Kudo Foundation, Nagoya-University Kyosaidann Research grant, Takeda Science Foundation, The Nitto Foundation, Kanae Foundation for the Promotion of Medical Science, Kowa Life Science Foundation, Shimadzu Foundation, Nakatani-Foundation, the Noguchi Institute, the Asahi Glass Foundation, the Ito Chubei Foundation, the Murata Science Foundation, Aichi Cancer Research Foundation, Toyoaki Scholarship Foundation, Suzuken Memorial Foundation, Research Grant of the Japan Cancer Society, Japanese Foundation for Multidisciplinary treatment of cancer, Japan Research Foundation for Clinical Pharmacology, Research grant of The Nagoya University Medical Association, Foundation for Promotion of Cancer Research. Funders only provided funding, and had no role in the study design, data collection, data analysis, interpretation, and writing of the report.

Declaration of interest

The authors declare no conflict of interest.

Author Contributions

The all authors checked and approved the final version of the manuscript. Y.I. and K.S. mainly conducted all experiments, performed analysis and wrote the manuscript; K.T., S.T., H.Y., Y.N., R.E., M.S., C.K., N.K., H.Y., Y.B., and Y.H. conducted analysis; S.N., T.F., K.K. and T.F.C.Y. conducted surgical operation to gather the specimens; K.S. supervised and conducted the project.

References

[1] William WN, Glisson BS. Novel strategies for the treatment of small-cell lung carcinoma. Nat Rev Clin Oncol 2011;8:611–9. https://doi.org/10.1038/nrclinonc.2011.90.

[2] Sabari JK, Lok BH, Laird JH, Poirier JT, Rudin CM. Unravelling the biology of SCLC: implications for therapy. Nat Rev Clin Oncol 2017;14. https://doi.org/10.1038/nrclinonc.2017.71.

[3] Siebel C, Lendahl U. Notch Signaling in Development, Tissue Homeostasis, and Disease. Physiol Rev 2017;97:1235–94. https://doi.org/10.1152/physrev.00005.2017.

[4] Sharma SK, Pourat J, Abdel-Atti D, Carlin SD, Piersigilli A, Bankovich AJ, et al. Noninvasive interrogation of DLL3 expression in metastatic small cell lung cancer. vol. 77. 2017.

https://doi.org/10.1158/0008-5472.CAN-17-0299.

[5] Saunders LR, Bankovich AJ, Anderson WC, Aujay MA, Bheddah S, Black K, et al. A DLL3-targeted antibody-drug conjugate eradicates high-grade pulmonary neuroendocrine tumor-initiating cells in vivo. Sci Transl Med 2015;7:302ra136-302ra136. https://doi.org/10.1126/scitranslmed.aac9459.

[6] Mitsunaga M, Ogawa M, Kosaka N, Rosenblum LT, Choyke PL, Kobayashi H. Cancer cell-selective in vivo near infrared photoimmunotherapy targeting specific membrane molecules. Nat Med 2011;17:1685–91. https://doi.org/10.1038/nm.2554.

[7] Sato K, Choyke PL, Hisataka K. Selective cell elimination from mixed 3D culture using a near infrared photoimmunotherapy technique. J Vis Exp 2016;2016:8–11. https://doi.org/10.3791/53633.

[8] Sato K, Nagaya T, Choyke PL, Kobayashi H. Near infrared photoimmunotherapy in the treatment of pleural disseminated NSCLC: Preclinical experience. Theranostics 2015;5:698–709. https://doi.org/10.7150/thno.11559.

[9] Sato K, Hanaoka H, Watanabe R, Nakajima T, Choyke PL, Kobayashi H. Near infrared photoimmunotherapy in the treatment of disseminated peritoneal ovarian cancer. Mol Cancer Ther 2014. https://doi.org/10.1158/1535-7163.MCT-14-0658.

[10] Sato K, Choyke PL, Kobayashi H. Photoimmunotherapy of gastric cancer peritoneal carcinomatosis in a mouse model. PLoS One 2014;9. https://doi.org/10.1371/journal.pone.0113276.

[11] Sato K, Nagaya T, Mitsunaga M, Choyke PL, Kobayashi H. Near infrared photoimmunotherapy for lung metastases. Cancer Lett 2015;365:112–21. https://doi.org/10.1016/j.canlet.2015.05.018.

[12] Sato K, Nagaya T, Nakamura Y, Harada T, Choyke PL, Kobayashi H. Near infrared photoimmunotherapy prevents lung cancer metastases in a murine model. Oncotarget 2015;6:19747–58. https://doi.org/10.18632/oncotarget.3850.

[13] Rudin CM, Pietanza MC, Bauer TM, Ready N, Morgensztern D, Glisson BS, et al. Rovalpituzumab tesirine, a DLL3-targeted antibody-drug conjugate, in recurrent small-cell lung cancer: a first-in-human, first-in-class, open-label, phase 1 study. Lancet Oncol 2017;18:42–51. https://doi.org/10.1016/S1470-2045(16)30565-4.

[14] Ramirez RD, Kurie J, Michael DiMaio J, Vaughan MB, Milchgrub S, Smith A, et al. O-205 Immortalization of normal human bronchial epithelial cells (NHBEC) in the absence of viral oncoproteins. Lung Cancer 2004;41:S60–1. https://doi.org/10.1016/s0169-5002(03)91863-0.

[15] Adachi T, Nonomura S, Horiba M, Hirayama T, Kamiya T, Nagasawa H, et al. Iron stimulates

plasma-activated medium-induced A549 cell injury. Sci Rep 2016;6:20928. https://doi.org/10.1038/srep20928.

[16] Hong W -S, Saijo N, Sasaki Y, Minato K, Nakano H, Nakagawa K, et al. Establishment and characterization of cisplatin-resistant sublines of human lung cancer cell lines. Int J Cancer 1988;41:462–7. https://doi.org/10.1002/ijc.2910410325.

[17] Minato K, Kanzawa F, Nishio K, Nakagawa K, Fujiwara Y, Saijo N. Characterization of an etoposide-resistant human small-cell lung cancer cell line. Cancer Chemother Pharmacol 1990;26:313–7. https://doi.org/10.1007/BF02897284.

[18] Kiura K, Watarai S, Ueoka H, Tabata M, Gemba KI, Aoe K, et al. An alteration of ganglioside composition in cisplatin-resistant lung cancer cell line. Anticancer Res 1998;18:2957–60.

[19] Takigawa N, Ohnoshi T, Ueoka H, Kiura K, Kimura I. Acta Medica Okayama Establishment and characterization of an etoposide-resistant human small cell lung cancer cell line. Acta Med Okayama 1992;46.

[20] Chikamori M, Takigawa N, Kiura K, Tabata M, Shibayama T, Segawa Y, et al. Establishment of a 7-ethyl-10-hydroxy-camptothecin-resistant small cell lung cancer cell line. Anticancer Res 2004;24:3911–6.

[21] Sato K, Watanabe R, Hanaoka H, Harada T, Nakajima T, Kim I, et al. Photoimmunotherapy: Comparative effectiveness of two monoclonal antibodies targeting the epidermal growth factor receptor. Mol Oncol 2014;8:620–32. https://doi.org/10.1016/j.molonc.2014.01.006.

[22] Saunders LR, Bankovich AJ, Anderson WC, Aujay MA, Bheddah S, Black K, et al. A DLL3-targeted antibody-drug conjugate eradicates high-grade pulmonary neuroendocrine tumor-initiating cells in vivo. Sci Transl Med 2015;7:302ra136-302ra136. https://doi.org/10.1126/scitranslmed.aac9459.

[23] Tanaka K, Isse K, Fujihira T, Takenoyama M, Saunders L, Bheddah S, et al. Prevalence of Delta-like protein 3 expression in patients with small cell lung cancer. Lung Cancer 2018;115:116–20. https://doi.org/10.1016/j.lungcan.2017.11.018.

[24] Sato K, Nakajima T, Choyke PL, Kobayashi H. Selective cell elimination in vitro and in vivo from tissues and tumors using antibodies conjugated with a near infrared phthalocyanine. RSC Adv 2015;5:25105–14. https://doi.org/10.1039/C4RA13835J.

[25] Puca L, Gavyert K, Sailer V, Conteduca V, Dardenne E, Sigouros M, et al. Delta-like protein 3 expression and therapeutic targeting in neuroendocrine prostate cancer. Sci Transl Med 2019;11. https://doi.org/10.1126/scitranslmed.aav0891.

[26] Owonikoko TK, Dahlberg SE, Sica GL, Wagner LI, Wade JL, Srkalovic G, et al. Randomized

phase II trial of cisplatin and etoposide in combination with veliparib or placebo for extensive-stage small-cell lung cancer: ECOG-ACRIN 2511 study. J Clin Oncol 2019;37:222–9. https://doi.org/10.1200/JCO.18.00264.

[27] Byers LA, Wang J, Nilsson MB, Fujimoto J, Saintigny P, Yordy J, et al. Proteomic profiling identifies dysregulated pathways in small cell lung cancer and novel therapeutic targets including PARP1. Cancer Discov 2012;2:798–811. https://doi.org/10.1158/2159-8290.CD-12-0112.

[28] Jhuraney A, Woods NT, Wright G, Rix L, Kinose F, Kroeger JL, et al. PAXIP1 potentiates the combination of WEE1 inhibitor AZD1775 and platinum agents in lung cancer. Mol Cancer Ther 2016;15:1669–81. https://doi.org/10.1158/1535-7163.MCT-15-0182.

[29] Sen T, Tong P, Diao L, Li L, Fan Y, Hoff J, et al. Targeting AXL and mTOR pathway overcomes primary and acquired resistance to WEE1 inhibition in small-cell lung cancer. Clin Cancer Res 2017;23:6239–54. https://doi.org/10.1158/1078-0432.CCR-17-1284.

[30] Makita S, Tobinai K. Targeting EZH2 with tazemetostat. Lancet Oncol 2018;19:586–7. https://doi.org/10.1016/S1470-2045(18)30149-9.

[31] Kim KH, Roberts CWM. Targeting EZH2 in cancer. Nat Med 2016;22:128–34. https://doi.org/10.1038/nm.4036.

[32] Schulze AB, Evers G, Kerkhoff A, Mohr M, Schliemann C, Berdel WE, et al. Future options of molecular-targeted therapy in small cell lung cancer. Cancers (Basel) 2019;11. https://doi.org/10.3390/cancers11050690.

[33] Thurston G, Noguera-Troise I, Yancopoulos GD. The Delta paradox: DLL4 blockade leads to more tumour vessels but less tumour growth. Nat Rev Cancer 2007;7:327–31. https://doi.org/10.1038/nrc2130.

[34] Furuta M, Kikuchi H, Shoji T, Takashima Y, Kikuchi E, Kikuchi J, et al. DLL3 regulates the migration and invasion of small cell lung cancer by modulating Snail. Cancer Sci 2019:1599–608. https://doi.org/10.1111/cas.13997.

[35] Deng SM, Yan XC, Liang L, Wang L, Liu Y, Duan JL, et al. The Notch ligand delta-like 3 promotes tumor growth and inhibits Notch signaling in lung cancer cells in mice. Biochem Biophys Res Commun 2017;483:488–94. https://doi.org/10.1016/j.bbrc.2016.12.117.

[36] Morgensztern D, Besse B, Greillier L, Santana-Davila R, Ready N, Hann CL, et al. Efficacy and Safety of Rovalpituzumab Tesirine in Third-Line and Beyond Patients with DLL3-Expressing, Relapsed/Refractory Small-Cell Lung Cancer: Results From the Phase II TRINITY Study. Clin Cancer Res 2019:1–10. https://doi.org/10.1158/1078-0432.ccr-19-1133.

[37] Kobayashi H, Choyke PL. Near-Infrared Photoimmunotherapy of Cancer. Acc Chem Res

2019:acs.accounts.9b00273. https://doi.org/10.1021/acs.accounts.9b00273.

[38] Sato K, Ando K, Okuyama S, Moriguchi S, Ogura T, Totoki S, et al. Photoinduced Ligand Release from a Silicon Phthalocyanine Dye Conjugated with Monoclonal Antibodies: A Mechanism of Cancer Cell Cytotoxicity after Near-Infrared Photoimmunotherapy. ACS Cent Sci 2018:acscentsci.8b00565. https://doi.org/10.1021/acscentsci.8b00565.

[39] Farago AF, Keane FK. Current standards for clinical management of small cell lung cancer. Transl Lung Cancer Res 2018;7:69–79. https://doi.org/10.21037/tlcr.2018.01.16.

[40] Sato K, Nagaya T, Mitsunaga M, Choyke PL, Kobayashi H. Near infrared photoimmunotherapy for lung metastases. Cancer Lett 2015;365:112–21. https://doi.org/10.1016/j.canlet.2015.05.018.

[41] Ito K, Mitsunaga M, Nishimura T, Saruta M, Iwamoto T, Kobayashi H, et al. Near-Infrared Photochemoimmunotherapy by Photoactivatable Bifunctional Antibody-Drug Conjugates Targeting Human Epidermal Growth Factor Receptor 2 Positive Cancer. Bioconjug Chem 2017;28:1458–69. https://doi.org/10.1021/acs.bioconjchem.7b00144.

[42] Ito K, Mitsunaga M, Arihiro S, Saruta M, Matsuoka M, Kobayashi H, et al. Molecular targeted photoimmunotherapy for HER2-positive human gastric cancer in combination with chemotherapy results in improved treatment outcomes through different cytotoxic mechanisms. BMC Cancer 2016;16:1–10. https://doi.org/10.1186/s12885-016-2072-0.

[43] Nagaya T, Nakamura Y, Sato K, Harada T, Choyke PL, Hodge JW, et al. Near infrared photoimmunotherapy with avelumab, an anti-programmed death-ligand 1 (PD-L1) antibody. Oncotarget 2016;8:8807–17. https://doi.org/10.18632/oncotarget.12410.

[44] Sato K, Sato N, Xu B, Nakamura Y, Nagaya T, Choyke PL, et al. Spatially selective depletion of tumor-associated regulatory T cells with near-infrared photoimmunotherapy. Sci Transl Med 2016;8. https://doi.org/10.1126/scitranslmed.aaf6843.

[45] Sato K, Watanabe R, Hanaoka H, Nakajima T, Choyke PL, Kobayashi H. Comparative effectiveness of light emitting diodes (LEDs) and Lasers in near infrared photoimmunotherapy. Oncotarget 2016;7:14324–35. https://doi.org/10.18632/oncotarget.7365.

[46] Okuyama S, Nagaya T, Sato K, Ogata F, Maruoka Y, Choyke PL, et al. Interstitial near-infrared photoimmunotherapy: effective treatment areas and light doses needed for use with fiber optic diffusers. Oncotarget 2018;9:11159–69. https://doi.org/10.18632/oncotarget.24329.

[47] Nagaya T, Okuyama S, Ogata F, Maruoka Y, Choyke PL, Kobayashi H. Endoscopic near infrared photoimmunotherapy using a fiber optic diffuser for peritoneal dissemination of gastric cancer. Cancer Sci 2018;109:1902–8. https://doi.org/10.1111/cas.13621.

[48] Nakajima K, Kimura T, Takakura H, Yoshikawa Y, Kameda A, Shindo T, et al. Implantable

wireless powered light emitting diode (LED) for near-infrared photoimmunotherapy: device development and experimental assessment *in vitro*and *in vivo*. Oncotarget 2018;9:20048–57. https://doi.org/10.18632/oncotarget.25068.

Figure Legends

Figure 1. Immunohistochemical staining of resected surgical specimens of SCLC, LCNEC, and carcinoid tumour cells.

(**a**) Hematoxylin-eosin and DLL3 staining in DLL3-negative SCLC cells and in DLL3-positive SCLC, LCNEC, lung carcinoid, and normal lung cells. Scale bars, 100 μm. (**b**) The table shows the number of DLL3-positive samples at our institute. One percent or more of the cells exhibited DLL3 staining in the membrane or cytoplasm at any intensity, and were considered DLL3-positive. LCNEC, large cell neuroendocrine carcinoma; SCLC, small cell lung cancer.

Figure 2. Confirmation of rova-IR700 conjugate construction and binding capacity.

(**a**) Validation of rova-IR700 by SDS-PAGE (left: colloidal blue staining, right: fluorescence at 700 nm). Diluted rovalpituzumab was used as a control.

(**b**) Immunoblotting with rova-IR700 in lysates from DLL3-overexpressing cells.

(**c**) Flow cytometric analysis of rova-IR700 in SBC3 and HBEC cells. DLL3 expression in SBC3 cells was evident, while fluorescence was essentially absent in the DLL3-negative HBEC human normal bronchial cells. Prior incubation with excess rovalpituzumab inhibited the binding of rova-IR700 to SBC3 cells, indicating that rova-IR700 binds specifically to DLL3.

Figure 3. DLL3 expressions in various cancer cell lines.

(**a**) Examination of DLL3 expression in SCLC cell lines established from Caucasian and Japanese SCLC patients.

(**b**) Examination of DLL3 expression in the chemoresistant SCLC cell lines, H69/CDDP, H69/VP, SBC3/CDDP, SBC3/ETP, and SBC3 /SN38. CDDP, cisplatin; ETP, etoposide; SCLC, small cell lung cancer; SN38, 7-ethyl-10-hydroxycamptothecin; VP, vePesid.

Figure 4. Effects of NIR-PIT with rova-IR700 on SCLC cell lines *in vitro*.

(**a**) Microscopic observations before and after DLL3-targeted NIR-PIT. DLL3-expressing SCLC cells were

incubated with rova-IR700 for 6 hours and observed with a microscope before and after irradiation with NIR light (4 J/cm^2). Necrotic cell death was observed after exposure to NIR light (20 minutes after NIR-PIT). Scale bars, 20 μm.

(**b**) Target cell- (SBC5-DLL3-luc-GFP) and non-target cell-expressing RFP (3T3-RFP, mouse fibroblasts) were co-cultured with rova-IR700 for 6 hours in the same dish and observed with a microscope before and after NIR light irradiation (4 J/cm^2). Selective targeted cell death was detected with Sytox Blue dead cell staining, while 3T3-RFP cells remain unchanged after exposure to NIR light (20 minutes after PIT). Scale bars, 20 μm.

(**c**) Membrane damage after DLL3-targeted NIR-PIT was measured by counting dead cells stained with propidium iodide, which increased in a light-dose dependent manner. Data are means ± SEMs ($n \geq 4$, *$p < 0.05$, **$p < 0.01$ [*t*-test]).

(**d**) Luciferase activity in SBC5-DLL3-luc-GFP and 3T3-DLL3-luc-GFP cells was measured in RLUs, which decreased in a NIR light dose-dependent manner. Data are means ± SEMs ($n \geq 3$, *$p < 0.05$, **$p < 0.01$ [*t*-test]). GFP, green fluorescent protein; NIR, near infrared; PIT, photoimmunotherapy; RFP, red fluorescent protein; RLU, relative light unit; SCLC, small cell lung cancer.

Figure 5. *In vivo* biodistribution of rova-IR700.

(**a**) Representative images before and after intravenous injection of rova-IR700 (fluorescence imager, 700 nm). The signal intensity on the tumour was increased up to 1 day post-injection and then gradually decreased until it was no longer detectable 7 days after injection. Signals in the bladder were observed at 0.5 hours after the injection, and liver accumulation was sustained through 1 day after injection. Scale bars, 20 mm.

(**b**) Fluorescence intensity measurement of the tumour and liver. Signal accumulation in the tumour was observed at 1 day after the injection. Data are means ± SEMs (n=3).

(**c**) The target-to-background ratio of the tumour and liver are indicated. Higher accumulation was observed in the tumour than in the liver 2–3 days after injection. Data are means ± SEMs (n=3).

(**d**) *Ex vivo* fluorescence imaging at 1 day after rova-IR700 injection. Specific accumulation in the tumour was observed in the injected mice. Tumours also showed bioluminescence (tu, tumour; he, heart; lu, lung; li, liver; pa, pancreas; sp, spleen; ki, kidney; st, stomach; in, intestine; bl, bladder.). Scale bars, 20 mm.

Figure 6. *In vivo* anti-tumour effect of DLL3-targeted NIR-PIT.

(**a**) DLL3-targeted NIR-PIT regimen involving rova-IR700 injection and NIR light exposure is shown in a line.

(**b**) *In vivo* fluorescence and the BLI of tumour-bearing mice. In the NIR-PIT group, fluorescence and luminescence was decreased after irradiation with NIR light. Scale bars, 20 mm.

(**c**) Tumour volume (mm^3) is shown in the left graph while the ratio is shown in the right (before NIR-PIT = 1). Prior to NIR-PIT, tumours were almost the same size. NIR-PIT introduced on days 0 and 1 led to significant reductions in the tumour volume ratio whereas neither rova-IR700 injection nor NIR light irradiation alone affected tumour size ($n \geq 7$ in each group.) (PIT group vs. control group at day 3: *p = 0.0212; PIT group vs. control group at day 7: *p = 0.0084; PIT group vs. light only group at day 7: *p = 0.0123; PIT group vs. light only group at day 10: *p = 0.0136; light only group vs. control group at day 3, 7, 10: $P > 0.9999$; i.v. only group vs. control group at day 3, 7, 10: $p > 0.9999$, Kruskal-Wallis test with Dunn's post-test).

(**d**) Quantitative RLU showed a significant decrease in DLL3-targeted NIR-PIT-treated tumours (n = 5 in each group) (PIT group vs. light-only group in (b): *p = 0.0007; PIT group vs. control group at (c): *p = 0.0385, Kruskal-Wallis test with Dunn's post-test).

(**e**) DLL3-targeted NIR-PIT led to prolonged survival in tumour-bearing mice ($n \geq 7$ in each group) (*p = 0.023, log-rank test).

(**f**) DLL3-targeted NIR-PIT regimen of SBC5-DLL3-luc-GFP xenografts in the dual-dorsal tumour mouse model.

(**g**) *In vivo* fluorescence and BLI of xenografts in the dual-dorsal tumour model. One day after rova-IR700 administration, only the tumour on the right was irradiated with NIR light. Fluorescence and luminescence were diminished only in the right tumour but not in the left. The site-specific effect *in vivo* was successfully performed. BLI, bioluminescence imaging; GFP, green fluorescent protein; NIR, near infrared; PIT, photoimmunotherapy; RLU, relative light unit. Scale bars, 20 mm.

Supplementary Information

Supplementary Figure 1.

DLL3 expression of cell line.

The 3T3 mouse fibroblast cells showed almost no florescence with rova-IR700 using flow cytometry.

Supplementary Figure 2.

Confirmation of DLL3, GFP, and luciferase expression in transfected cells. lines. Expression of GFP and DLL3 in transfected cells were stronger than in their wild-type counterparts (A) SBC5-DLL3-luc-GFP

(B) 3T3-DLL3-luc-GFP. Luciferase expression was confirmed with luminescence gradually increased as cells proliferated. Over 10 passages were performed to obtain stable expression. GFP, green fluorescent protein.

Supplementary Figure 3.

Weight changes in treated mice.

The weights of the mice remained within the same range throughout the experimental period.

Supplementary Video.

(**1**) Time-lapse images of SBC5-DLL3-luc-GFP (**1a**) and 3T3-DLL3-luc-GFP (**1b**) treated with NIR-PIT. The video shows rapid membrane damage in both cells treated with rova-IR700 after NIR light irradiation, as confirmed with propidium iodide staining (20 minutes observation in total). The flashing light is the NIR light irradiation (4 J/cm^2).

(**2**) Time-lapse images of SBC5-DLL3-luc-GFP (target cell) and 3T3-RFP (non-target cell) treated by NIR-PIT. The DLL3 expressing target cell shows IR700 fluorescence before NIR light irradiation. NIR-PIT only damages the DLL3 expressing cell while the non-target cell stays intact, as confirmed with propidium iodide and Sytox Blue dead cell staining (20 minutes observation in total). The flashing light is the NIR light irradiation (4 J/cm^2). GFP, green fluorescent protein; NIR, near infrared; PIT, photoimmunotherapy; RFP, red fluorescent protein.

Figure 1

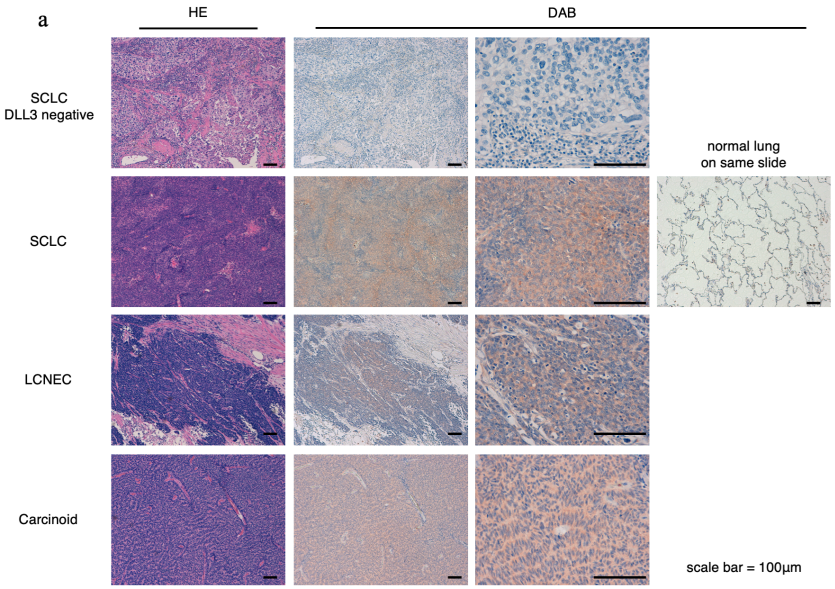

b

Number of DLL3 positive (1% <) samples

SCLC	LCNEC	Carcinoid
8 / 10	5 / 10	8 / 8

Figure 2

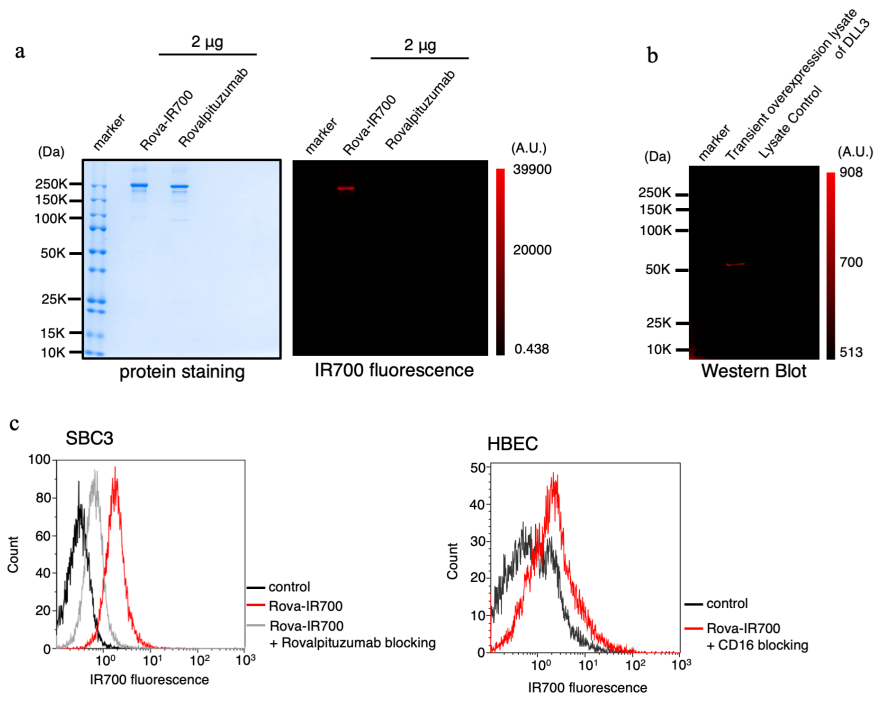
a
2 µg
2 µg
marker
Rova-IR700
Rovalpituzumab
(Da)
250K
150K
100K
50K
25K
15K
10K
protein staining
IR700 fluorescence
(A.U.)
39900
20000
0.438
b
Transient overexpression lysate of DLL3
Lysate Control
908
700
513
Western Blot
c
SBC3
HBEC
Count
IR700 fluorescence
control
Rova-IR700
Rova-IR700
+ Rovalpituzumab blocking
+ CD16 blocking

Figure 3

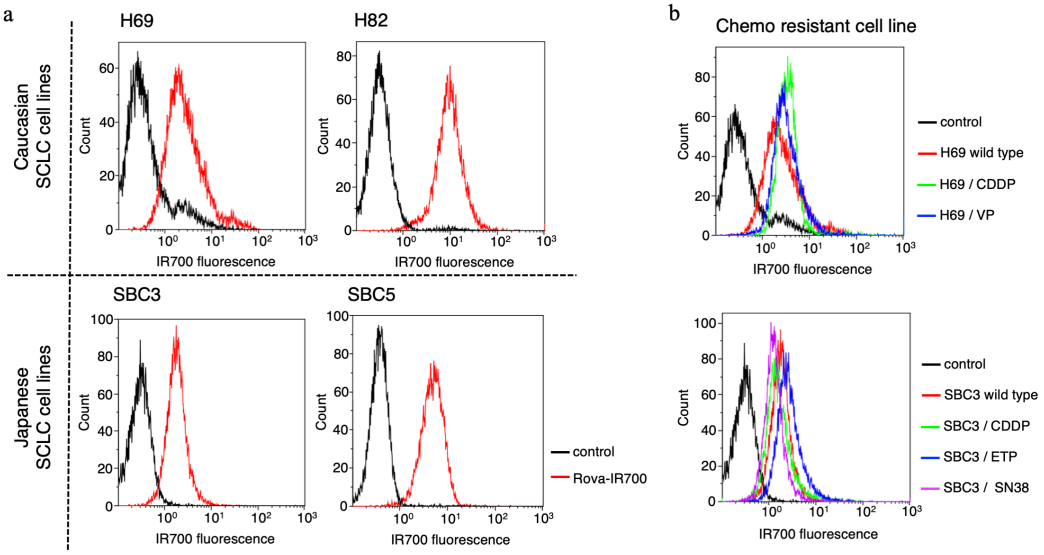
a
H69
H82
Caucasian SCLC cell lines
Count
IR700 fluorescence
SBC3
SBC5
Japanese SCLC cell lines
control
Rova-IR700
b
Chemo resistant cell line
control
H69 wild type
H69 / CDDP
H69 / VP
control
SBC3 wild type
SBC3 / CDDP
SBC3 / ETP
SBC3 / SN38

Figure 4

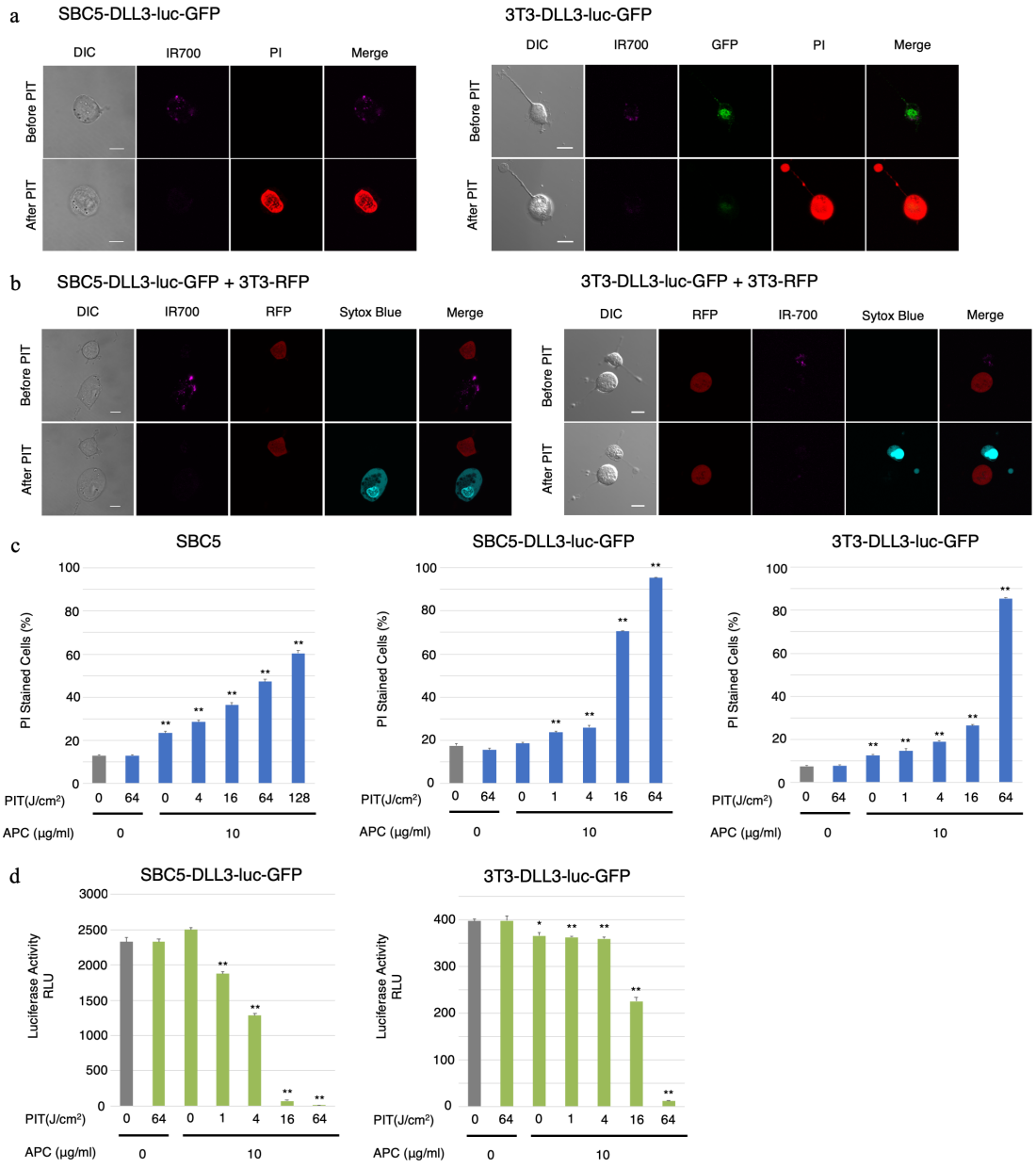
a
SBC5-DLL3-luc-GFP
DIC
IR700
PI
Merge
Before PIT
After PIT
3T3-DLL3-luc-GFP
DIC
IR700
GFP
PI
Merge
Before PIT
After PIT
b
SBC5-DLL3-luc-GFP + 3T3-RFP
DIC
IR700
RFP
Sytox Blue
Merge
Before PIT
After PIT
3T3-DLL3-luc-GFP + 3T3-RFP
DIC
RFP
IR-700
Sytox Blue
Merge
Before PIT
After PIT
c
SBC5
SBC5-DLL3-luc-GFP
3T3-DLL3-luc-GFP
PI Stained Cells (%)
PIT(J/cm²)
APC (μg/ml)
0 64 0 4 16 64 128
0 64 0 1 4 16 64
0
10
d
SBC5-DLL3-luc-GFP
3T3-DLL3-luc-GFP
Luciferase Activity RLU
PIT(J/cm²)
APC (μg/ml)
0 64 0 1 4 16 64
0
10

Figure 5

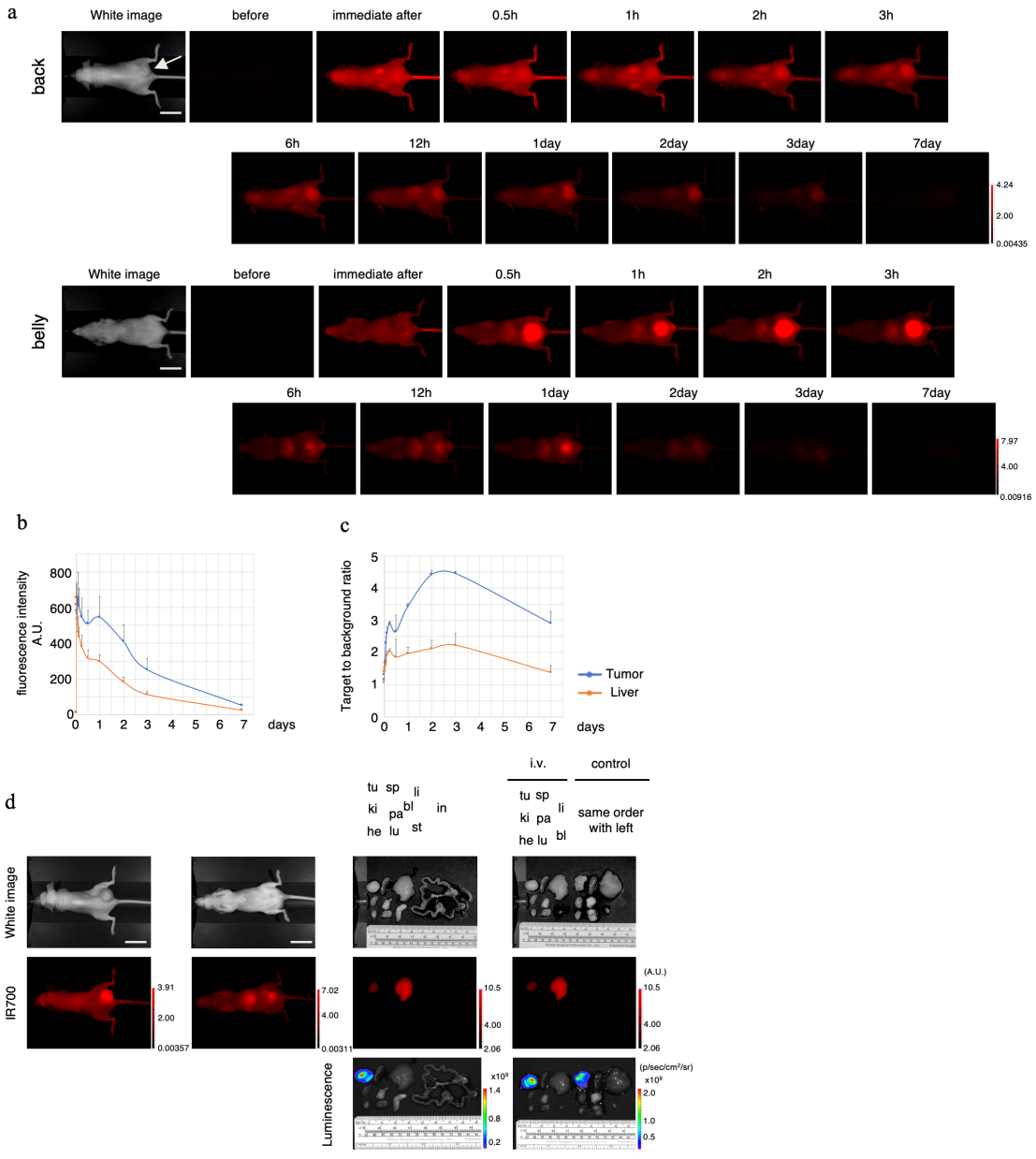
a
White image
before
immediate after
0.5h
1h
2h
3h
back
6h
12h
1day
2day
3day
7day
4.24
2.00
0.00435
White image
before
immediate after
0.5h
1h
2h
3h
belly
6h
12h
1day
2day
3day
7day
7.97
4.00
0.00916
b
fluorescence intensity A.U.
800
600
400
200
0
0 1 2 3 4 5 6 7
days
c
Target to background ratio
5
4
3
2
1
0
0 1 2 3 4 5 6 7
days
Tumor
Liver
d
i.v.
control
tu sp li
ki pa bl in
he lu st
tu sp li
ki pa bl
he lu
same order with left
White image
IR700
3.91
2.00
0.00357
7.02
4.00
0.00311
10.5
4.00
2.06
(A.U.)
10.5
4.00
2.06
Luminescence
x10⁹
1.4
0.8
0.2
(p/sec/cm²/sr)
x10⁹
2.0
1.0
0.5

Figure 6

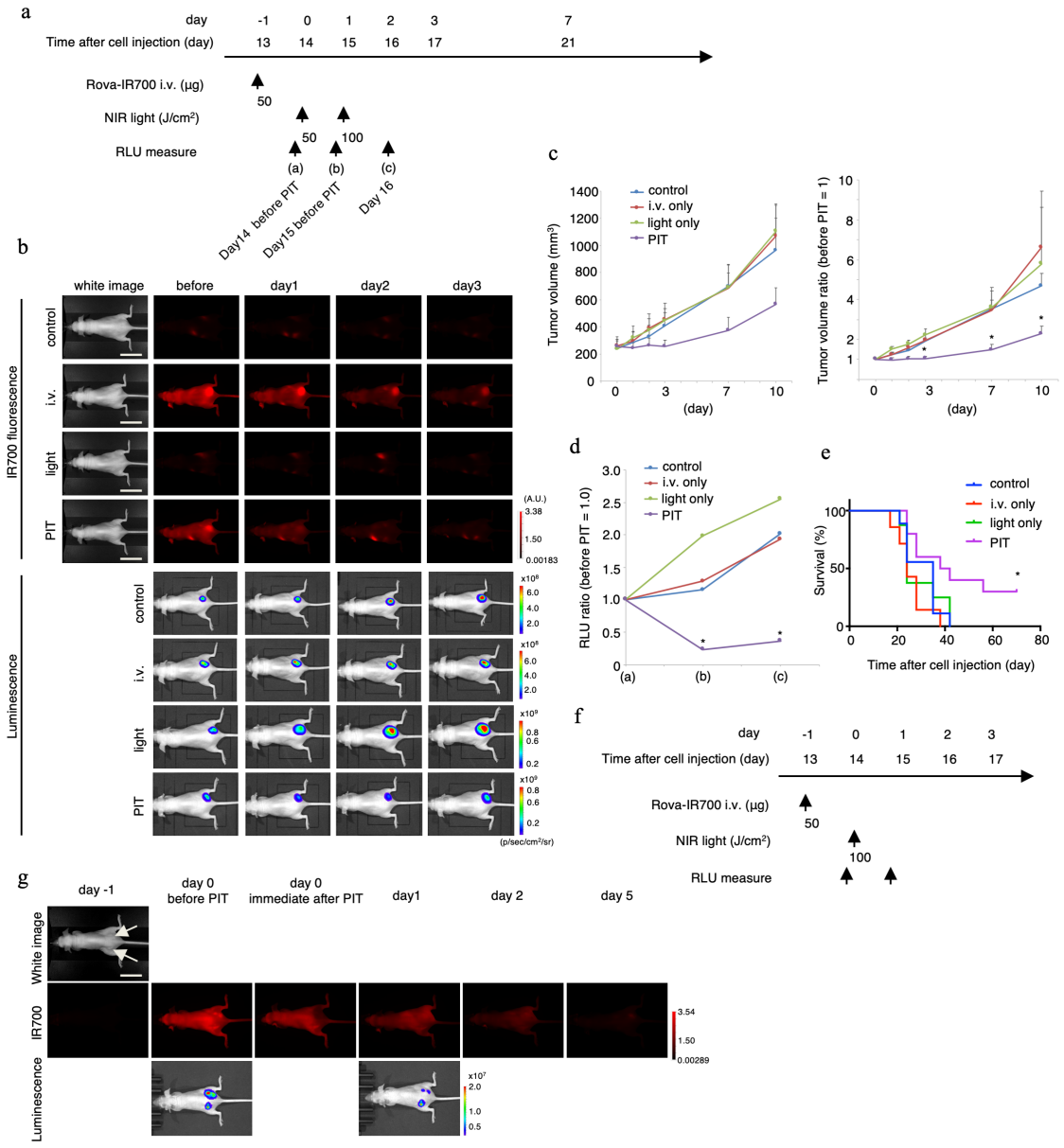
a
day
Time after cell injection (day)
Rova-IR700 i.v. (μg)
NIR light (J/cm²)
RLU measure
Day14 before PIT
Day15 before PIT
Day 16
b
white image
before
day1
day2
day3
IR700 fluorescence
Luminescence
control
i.v.
light
PIT
(p/sec/cm²/sr)
c
Tumor volume (mm³)
Tumor volume ratio (before PIT = 1)
control
i.v. only
light only
PIT
(day)
d
RLU ratio (before PIT = 1.0)
e
Survival (%)
Time after cell injection (day)
f
g
day -1
day 0 before PIT
day 0 immediate after PIT
day1
day 2
day 5
White image
IR700
Luminescence